

# Use of phase-locking value in sensorimotor rhythm-based brain–computer interface: zero-phase coupling and effects of spatial filters

Wenjuan Jian<sup>1,2</sup>  · Minyou Chen<sup>1</sup> · Dennis J. McFarland<sup>2</sup>

Received: 10 September 2016 / Accepted: 17 March 2017  
© International Federation for Medical and Biological Engineering 2017

**Abstract** Phase-locking value (PLV) is a potentially useful feature in sensorimotor rhythm-based brain–computer interface (BCI). However, volume conduction may cause spurious zero-phase coupling between two EEG signals and it is not clear whether PLV effects are independent of spectral amplitude. Volume conduction might be reduced by spatial filtering, but it is uncertain what impact this might have on PLV. Therefore, the goal of this study was to explore whether zero-phase PLV is meaningful and how it is affected by spatial filtering. Both amplitude and PLV feature were extracted in the frequency band of 10–15 Hz by classical methods using archival EEG data of 18 subjects trained on a two-target BCI task. The results show that with right ear-referenced data, there is meaningful long-range zero-phase synchronization likely involving the primary motor area and the supplementary motor area that cannot be explained by volume conduction. Another novel finding is that the large Laplacian spatial filter enhances the amplitude feature but eliminates most of the phase information seen in ear-referenced data. A bipolar channel using phase-coupled areas also includes both phase and amplitude

information and has a significant practical advantage since fewer channels required.

**Keywords** Brain–computer interface (BCI) · Phase-locking value (PLV) · Spatial filters · Zero phase

## 1 Introduction

A brain–computer interface (BCI) provides a novel communication channel to help those who are unable to generate useful muscular movements, control devices or communicate with the external environment [47]. Phase synchrony is a popular choice as a BCI control signal. However, there is a potential problem for the interpretation of phase synchrony since the activity at any pair of electrodes could be due both to connectivity between distant sources and to volume conduction (i.e., the conductive properties of the tissue through which the EEG propagates causes the spatial smearing of signals).

Measures such as the phase-locking index (PLI) [31, 39] and the imaginary part of coherence [28] are intended to eliminate the effects of volume conduction by negating effects near zero-phase lag [28, 39]. However, neither of these measures are pure indices of phase-coupling strength because: the imaginary part of coherence is influenced by both the amplitude of the signal and phase delay [31, 39]; PLI is not completely independent of volume conduction effects [31]. In addition, while larger PLI indicates stronger non-zero phase locking, it may be the case that not all zero-phase coupling is due to volume conduction [8, 46]. Both coherence [18, 29, 30, 33] and phase-locking value (PLV) [16, 38] can be used to estimate the degree of phase synchrony. Coherence (a frequency-domain measure) is the cross-spectral

---

**Electronic supplementary material** The online version of this article (doi:10.1007/s11517-017-1641-y) contains supplementary material, which is available to authorized users.

---

✉ Wenjuan Jian  
mofeixiju@gmail.com; wenjuanjian@126.com

<sup>1</sup> State Key Laboratory of Power Transmission Equipment and System Security and New Technology, School of Electrical Engineering, Chongqing University, Chongqing 400044, China

<sup>2</sup> National Center for Adaptive Neurotechnologies, Wadsworth Center, New York State Department of Health, Albany, NY, USA

density function normalized by the auto-spectral density functions of the individual channels. It is sensitive to the magnitude of both time series and the consistency of their phase relationships [16]. PLV is a function of pure phase difference and assess the phase-coupling strength independent of amplitude. Therefore, we used PLV in this study.

It is not clear from the literature whether or not to use spatial filtering when evaluating phase coupling. Speigler et al. [38] used a finite impulse response (FIR) band-pass between 8 and 12 Hz and a common average reference (CAR) and convolved the resulting signal with a complex Gabor/Morlet wavelet to compute PLV. Zhou et al. [48] used a large Laplacian (LL) followed by empirical mode decomposition (EMD) [10, 13] and a Hilbert transformation. Investigators have used a variety of reference [43, 44] (e.g., POz reference, ear reference) and re-referencing [45] techniques (e.g., CAR reference) to study PLV. There are at least two problems with the choice of reference. Any activity in a reference will be common to all other electrodes. In addition, re-referencing, as with CAR [45] and large Laplacian [48] has spatial filtering effects. Andrew and Pfurtscheller [2] and Florian et al. [11] argue for the use of spatial filtering when examining coupling because spatial filtering reduces the effects of volume conduction and better reflects the activity of local sources. Tenke and Kayser [41] also state that it is better to apply a surface Laplacian when studying coherence. In contrast, Brunner et al. [6] recommend not applying spatial filtering when using PLV as a control feature in BCI.

Since a large Laplacian was shown to improve target prediction ability based on the square root of band power (BP) [20], in this study, the PLV extracted using monopolar data (i.e., no spatial filter applied, monopolar condition) and data after preprocessing by large Laplacian (Laplacian condition) were compared. BP feature was also studied in the present study in order to aid the understanding of the effects of spatial filters on phase synchrony.

Krusienski et al. [15] stated that phase did not add information in addition to that provided by amplitude. But they did not examine C3/C4 coupling with FCz. Wei et al. [45] found that combining PLV and amplitude could effectively improve the classification accuracy. Our result will show that this largely depends on the way we compute PLV feature (i.e., in Laplacian or monopolar condition) and the coupling locations that were chosen for computing PLV. Previous studies of amplitude and phase have suggested that phase synchrony should increase with increasing amplitude [5, 9] due to an improvement in signal-to-noise ratio (SNR). In this context, if there is noise in a channel, then increasing the amplitude of the signal should improve the SNR and hence increase PLV. We will show that the amplitude and PLV feature at zero-phase difference vary in

opposite directions with monopolar data. This is contrary to what would be expected based on volume conduction.

## 2 Methods

### 2.1 Experiment paradigm and data recording

Eighteen individuals (10 males and 8 females), aged 27–60 years ( $M = 38.06$ ,  $SD = 10.90$ ), participated in this study. All subjects gave informed consent for the study, which was reviewed and approved by the New York State Department of Health Institutional Review Board. EEG recording was performed with subjects seated comfortably in a reclining chair facing a 51 cm video screen 3 m away. Subjects were asked to remain motionless during performance. The data were recorded using BCI2000 software [34] in conjunction with a 64-channel SA instrumentation amplifier and a Data Translation DT-3003 64 channel A/D board, to collect EEG activity from 64 channels distributed over the scalp at standard locations [35]. We used 9-mm tin electrodes embedded in a cap (Electro-Cap International). All channels were referenced to the right ear, band-pass filtered (0.1–60 Hz) and digitized at a sampling of 160 Hz.

All users were trained on a simple two-target, one-dimensional cursor control task, with the standard online protocol detailed in [15, 23]. The targets appear on either the top half or bottom half of the right-edge of the screen. The users goal was to control the cursor in order to hit the top or bottom target by the combination of amplitude of one or several locations or electrodes in sensorimotor cortex, calculated from the 3–4 Hz wide bins in a  $\mu$  ([9, 15] Hz) or beta-rhythm band ([20, 25] Hz) according to the linear function that determined each cursor movement:

$$\Delta V = b(S - a), \quad (1)$$

where  $\Delta V$  was the cursor movement,  $S$  was the control signal [e.g., a linear sum of the spectral band-channel combinations (one or more features)],  $b$  was the gain, operated at the end of each 3-min run [24] and  $a$  was the mean control signal ( $S$ ) for the user's previous performance [21]. The  $b$  and  $a$  in Eq. (1) were adjusted independently to eliminate any correlation between the probability that the target would be hit and the vertical location of the target in order to ensure that all targets (i.e., upward or downward) were equally accessible. The control signal  $S$  in Eq. (1) can be expressed in terms of its constituent features (i.e.,  $\mu$  or beta-rhythm amplitudes) as

$$S = \sum w_i x_i, \quad (2)$$

where  $x_i$  is the  $i$ th feature and  $w_i$  is the weight given to that feature based on prior data.

Each user completed 2–3 sessions per week. After ten sessions training, users learned to increase or decrease the spectral amplitude in mu or beta-rhythm band. The data from the last training session was used for off-line analysis in this paper. For 17 subjects, this session consisted of 8 runs (mostly around 3 min) separated by 1 min breaks and each run consisted of 20–30 trials. For one subject, only 6 runs were completed in this session. Across all subjects, the average number of trials for each task was  $98.66 \pm 13.8$ , and each trial lasted about 3–4 s.

The frequency used online for the 18 subjects was most often centered at 13 Hz (only 6 were focused in beta range). Therefore, in this article, we extracted the PLV and BP feature in [10, 15] Hz. Since the direction of cursor movement produced by sensorimotor rhythm (SMR) desynchronization was programmed differently in different subjects, we sorted the data of each subject so that task 1 required BP increase and task 2 required BP decrease based on the monopolar EEG signal at C3 in the frequency range of [10, 15] Hz. Linear interpolation was applied to correct for phase differences caused by the sequential digitization of channels [22].

### 2.2 Feature extraction

Despite the fact that phase synchrony might be formally extended for an arbitrary broad-band signal, a clear physical meaning may only make sense for narrow-band signals [17]. Therefore, we applied filtration to isolate the frequency band of interest from the background brain activity using an FIR type I with a band-pass of 10–15 Hz realized by Matlab *fir1* (with hamming window applied) and *filter* functions. FIR order was computed according to the formula,

$$\text{Order} = N_{\text{cycle}} * f_s / f_1, \tag{3}$$

where  $N_{\text{cycle}}$  is the number of cycles,  $f_s$  corresponds to the sampling rate and  $f_1$  is the lower frequency bound in the band  $[f_1, f_2]$  (e.g., [10, 15] Hz was chosen and  $f_1 = 10$  in this study). The results are robust when  $N_{\text{cycle}}$  ranges from 4 to 6. In this article, only the results of  $N_{\text{cycle}} = 5$  (sum of squared errors, SSE = 0.35) were presented. We applied the filter FIR and Hilbert transformation to compute PLV since it was reported that there is no significant difference between wavelet and Hilbert transform for determination of phase with scalp EEG signals [17].

The PLV feature can be calculated from short data segments to ensure quasi-stationary [45]. We computed both features by segmenting the data into 400 ms segments every 50 ms (in the same manner as amplitude features for online cursor movement were determined) and by using the whole trial of data (around 3–4 s). Either method of computing

PLV shows similar results. In this article, we presented the result based on the whole trial data:

$$\text{PLV} = \left| \frac{1}{N} \sum_{n=1}^N e^{j(\varphi_x(n) - \varphi_y(n))} \right|, \tag{4}$$

where  $N$  is the total number of data points for each trial,  $\varphi_x(n) - \varphi_y(n)$  is the instantaneous phase difference between of EEG signals of channel  $x$  and  $y$ .

Hilbert transformation was applied in determining the instantaneous phase of EEG signals:

$$y_i(t) = \frac{1}{\pi} P \int_{-\infty}^{+\infty} \frac{u_i(\tau)}{t - \tau} d\tau, i = 1, 2, \dots, n, \tag{5}$$

$$\varphi_i(t) = \arctan \frac{y_i(t)}{u_i(t)}, \tag{6}$$

where  $u_i(t)$  is the EEG signal after preprocessing (e.g., FIR or spatial filtering + FIR) and  $P$  denotes the Cauchy principle value.

The root mean square value (RMS) was computed with the FIR filtered signal, which can be considered as the BP feature in the frequency band  $[f_1, f_2]$  ([10, 15] Hz).

### 2.3 Evaluation and statistical significance tests

Both PLV and BP were measured under monopolar and Laplacian conditions. We evaluated user’s EEG control with  $r$  or  $r^2$  [36], the proportion of the total variance in EEG feature that was accounted for by different target positions. The  $r$  value based on BP and PLV feature being applied to show the direction of increase or decrease in task 2 compared with task 1 was computed by:

$$r = \frac{\sum_{i=1}^n (x_i - \bar{x})(y_i - \bar{y})}{\sqrt{\sum_{i=1}^n (x_i - \bar{x})^2} \sqrt{\sum_{i=1}^n (y_i - \bar{y})^2}}, \tag{7}$$

where the vector  $x_1, \dots, x_n$  containing  $n$  values corresponding to the BP or PLV feature values,  $\bar{x} = \frac{1}{n} \sum_{i=1}^n x_i$  and another vector  $y_1, \dots, y_n$  containing  $n$  values corresponding to the task label (e.g., +1 for top (task 1) and -1 for bottom (task 2) targets),  $\bar{y} = \frac{1}{n} \sum_{i=1}^n y_i$ . Multiple linear regression was used for computing the  $r^2$  value based on combined BP and PLV feature.

For statistical tests, the dependent variable for different features (BP, PLV or the combined feature of BP and PLV) was  $r^2$ .

Data analysis was performed off-line with Matlab2014 and all statistic tests were done with the SAS statistical software (SAS Institute Inc., Cary, NC). Repeated analysis of variance (ANOVA) was used to evaluate the effects of features (e.g., PLV features for different coupled channels),

and target position (task 2 versus task 1) on target prediction abilities ( $r^2$  based on BP, PLV and combined feature,  $r_{BP}^2, r_{PLV}^2, r_{CF}^2$ ) and data derivations (e.g., monopolar condition, Laplacian condition). Means for ANOVA effects that were significant were compared with Tukey’s adjustment for multiple comparisons. We used an alpha level of  $p < 0.05$  to describe statistical significance. Before applying repeated ANOVA, Mauchly’s sphericity test was applied. If the sphericity assumption was violated, the  $p$  values and the degrees of freedom of all repeated measures ANOVAs were adjusted by the method of Greenhouse–Geisser (the estimate of sphericity was  $<0.75$ ).

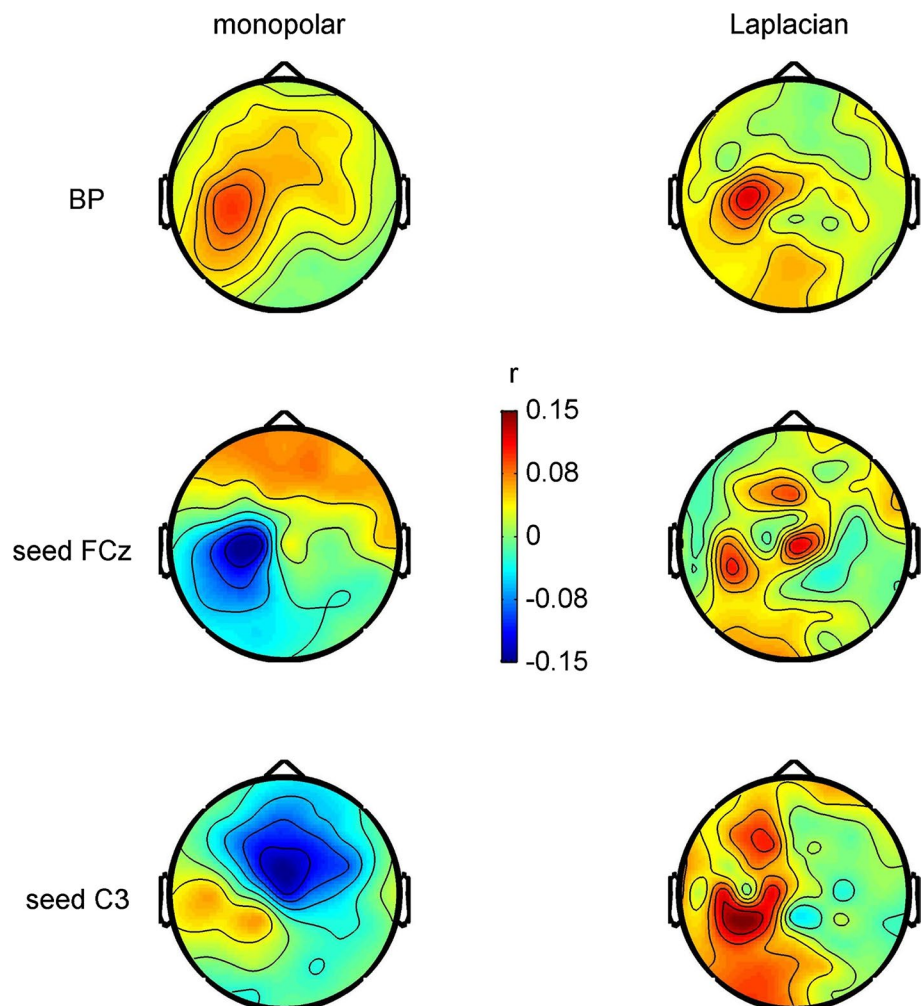
### 3 Results

#### 3.1 PLV and BP features in monopolar and Laplacian conditions

We computed the  $r_{BP}$  (vector of  $1 \times 64$ ) of all channels and found that the largest absolute  $r_{BP}$  value corresponded

to channel C3. We also computed  $r_{PLV}$  (a matrix of  $64 \times 64$ , by treating all 64 channels as seed channels, respectively) of all PLV couplings and found the best pair of channels to be C3 coupling with FCz. Figure 1 shows the  $r_{BP}$  (top row) and  $r_{PLV}$  (middle and bottom rows with PLV being computed by all other 63 channels coupled with seed channels FCz and C3, respectively) based topographies. The left column shows the monopolar condition, and the right column shows the Laplacian condition. Figure 1 top left panel shows that for all subjects the amplitude feature at 10–15 Hz in task 2 is smaller than that in task 1, indicating event-related desynchronization (ERD) on the left side. However, the middle and bottom left panels show that PLV between C3 and FCz in task 2 is larger than that in task 1. Therefore, the monopolar condition (Fig. 1 left column) shows that the BP and PLV vary in opposite directions during the cursor control task [BP is located in the vicinity of the primary motor area (M1) and PLV represents coupling between electrodes near M1 and the supplementary motor area (SMA)].

**Fig. 1** Opposite modulation between BP (C3 area) and PLV (FCz coupling with C3). *Left and right columns* show the topographies of  $r_{BP}$  (top row)  $r_{PLV}$  (middle and bottom rows) in monopolar and Laplacian conditions, respectively, of task 2 versus task 1. Both BP and PLV feature were evaluated between 10 and 15 Hz. PLV were measured by referring to seed channel FCz (middle row) and C3 (bottom row) channels, respectively

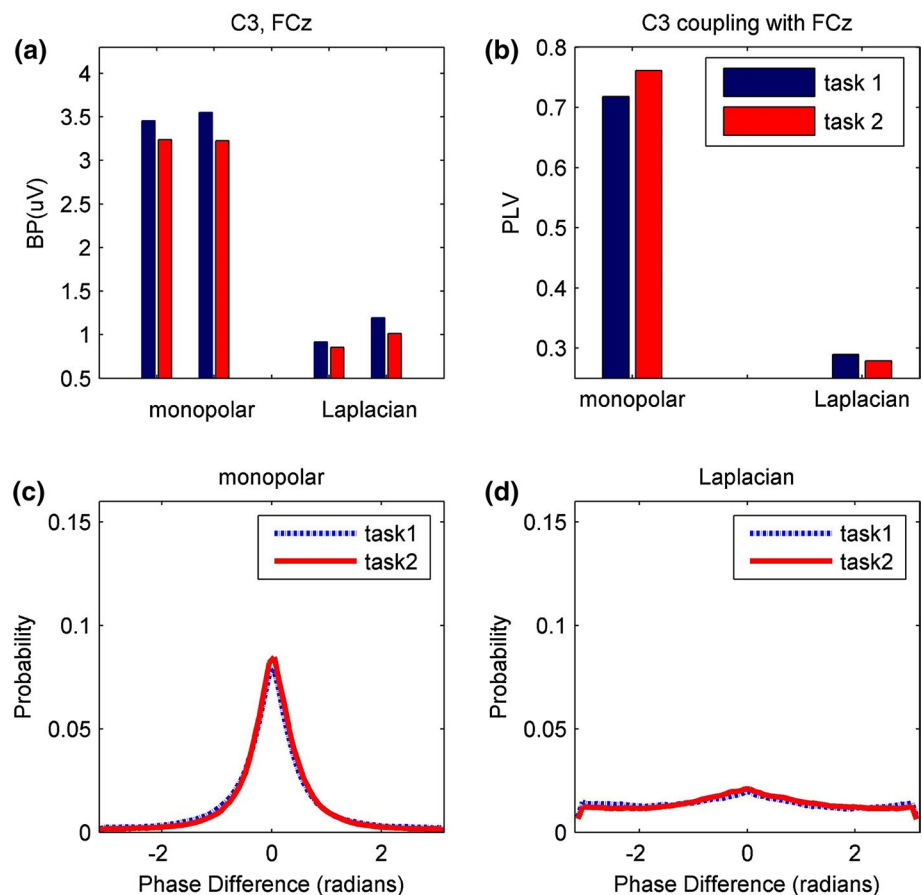


Spatial filtering is a common preprocessing operation in EEG analysis. Using simulations, Tenke and Kayser [41] showed that the surface Laplacian enhanced results for both amplitude and phase coupling (coherence). However, simulation results are limited to the manner in which EEG is modeled and must be evaluated by how well they explain empirical studies. As discussed earlier, Brunner et al. [6] recommended the use of monopolar EEG when using PLV as a control feature. Figure 1 (top right panel) also shows that when large Laplacian is applied, the correlation of BP with target position is increased at C3 area comparing with the corresponding  $r_{BP}$ -based topography of monopolar condition (Fig. 1 top left panel). This effect is consistent with previous studies [20, 22], indicating that the Laplacian method improves target prediction. However, the effect of target position on phase coupling between C3 and FCz is markedly reduced (Fig. 1 middle and bottom right panels) comparing with that in the monopolar condition (Fig. 1 middle and bottom left panels).

We next did a statistical evaluation of amplitude at FCz and C3 and PLV between C3 and FCz in both conditions. Two-way repeated ANOVA based on BP feature in each condition shows that there is no significant interaction between channel location (two levels: C3 and FCz)

and task condition (two levels: task 1 and task 2) in both monopolar and Laplacian condition. However, BP features of C3 and FCz in both conditions decrease in task 2 compared with that in task 1 ( $F(1, 17) = 32.55, p < 0.0001$  and  $F(1, 17) = 10.15, p < 0.0054$ , respectively, Fig. 2a). For the PLV feature (Fig. 2b), a repeated one-way ANOVA shows that PLV in task 2 is significant larger than that in task 1 ( $F(1, 17) = 6.86, p < 0.018$ ) in monopolar condition. However, there is no significant difference between PLV in task 1 and that in task 2 in Laplacian condition. Figure 2a, b shows that there is opposite modulation between BP (C3) and PLV (C3 coupling with FCz) in monopolar condition. This opposite modulation is not due to the phenomenon of “focal ERD/surround ERS” [32] since ERD occurs at both electrodes. However, when a large Laplacian was applied, the phase feature was reduced so that the opposite modulation between BP and PLV did not occur. The phase difference probability density distribution (Fig. 2c, d) shows that C3 and FCz were phase-locked mainly at zero-phase difference for both tasks. However, the phase difference distribution is much flatter when a large Laplacian was applied (Fig. 2d) as compared to the distribution for the monopolar condition (Fig. 2c).

**Fig. 2** The BP and phase feature in monopolar and Laplacian conditions. **a** Amplitude feature (BP) for task 1 and task 2 of C3 and FCz channels in both conditions. **b** PLV feature for task 1 and task 2 between C3 and FCz channel in monopolar and Laplacian conditions. **c, d** The phase difference distribution between C3 and FCz in task 1 and task 2 in monopolar and Laplacian condition, respectively



Since C3 and FCz were phase-locked near zero-phase difference for all subjects (Fig. 2c), there is a distinct possibility that the phase coupling (PLV) between C3 and FCz was due to volume conduction rather than to long-distance connectivity between the tissue near these recording sites. The large Laplacian is expected to decrease the effects of volume conduction [2, 11]. However, volume conduction would not produce modulation of amplitude and phase coupling in opposite directions (Fig. 2a, b monopolar condition).

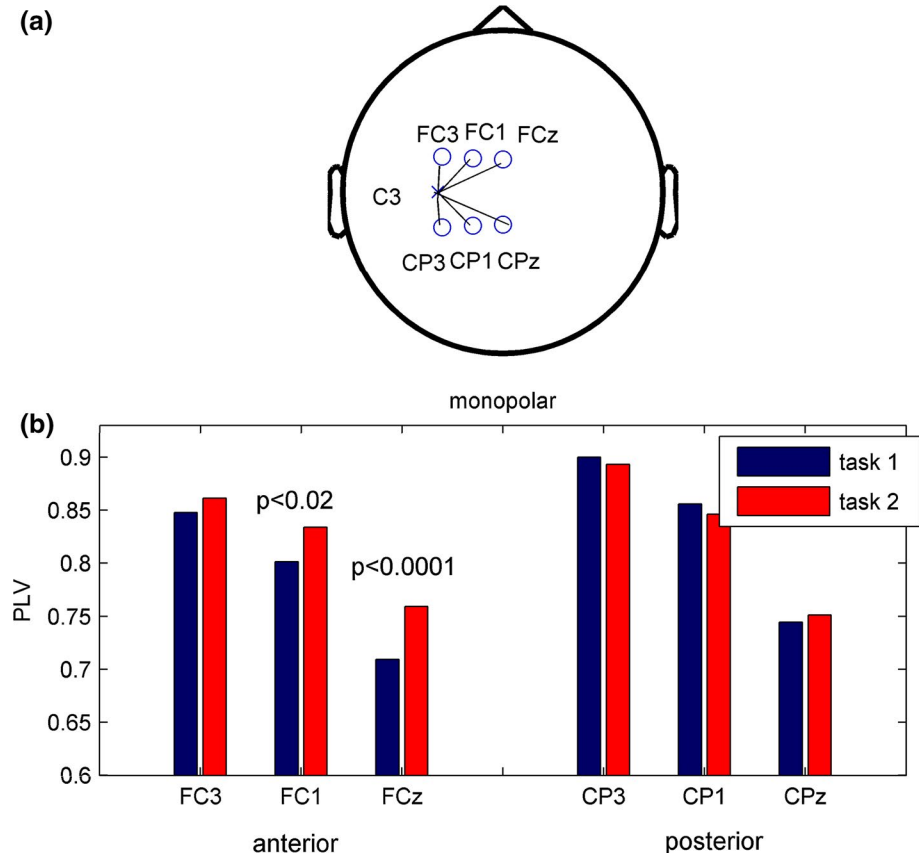
To further explore functional connectivity between C3 and FCz, we compared the PLV feature of task 1 and task 2 for C3 coupled with FC3, FC1 and FCz and contrasted this with coupling of C3 with CP3, CP1, and CPz (Fig. 3a) in the monopolar condition. A repeated measures ANOVA resulted in a significant interaction between electrode location (e.g., anterior: FC3, FC1, FCz; posterior: CP3, CP1, CPz) and task condition (e.g., task 1 and task 2) ( $F(1.447, 24.599) = 7.09, p < 0.0073$  corrected from  $F(5, 85) = 7.09, p < 0.0001$ ). Figure 3b shows two effects. As the lateral to medial distance between C3 increases, PLV decreases (coupling of C3 and FC3 > FC1 > FCz; coupling of C3 and CP3 > CP1 > CPz). This effect of distance is consistent with volume conduction which should decrease with distance. In addition, there is a second trend in which

the anterior electrodes FC1 and FCz show a greater task-related effect than the posterior electrodes (e.g., CP1 and CPz). Here, C3 coupling with FC1, and FCz is greater for task 2 than task 1 ( $p < 0.02$  and  $p < 0.0001$ , respectively, by Tukey's post hoc test). In contrast, C3 coupling with CP1, and CPz was not significantly different between tasks 1 and 2. This effect of task, present in anterior electrodes (FC1, FCz) and absent in posterior electrodes (CP1, CPz), would not be predicted on the basis of volume conduction. Thus, the phase locking effects shown in Fig. 3 were the result of the superposition of two effects: volume conduction and long-distance coupling between motor and premotor sites. This indicates that the PLV between C3 and FCz is meaningful in the monopolar condition, and that after applying a large Laplacian, the PLV feature was altered (Fig. 2b, d).

### 3.2 Target prediction ability based on PLV and BP in both monopolar and Laplacian conditions

Given that BP and PLV were modulated in opposite directions by target position in the monopolar condition and that PLV was reduced in the Laplacian condition, we next further explored the effects of spatial filtering. To this end, we examined the prediction of target location by PLV ( $r_{PLV}^2$ )

**Fig. 3** **a** The electrodes layout that involves C3, anterior (e.g., FC3, FC1, FCz), and posterior electrodes (e.g., CP3, CP1, CPz). **b** There is significant interaction between task and channel location at  $F(1.447, 24.599) = 7.09, p < 0.0073$  with Greenhouse–Geisser correction. PLV of C3 coupling with FC1 and FCz is greater for task 2 than task 1 ( $p < 0.02$  and  $p < 0.0001$ , respectively) by Tukey's post hoc test



of PLV coupling between C3 and FCz), BP ( $r_{BP}^2$  of BP at C3), as well as PLV and BP combined ( $r_{CF}^2$ ) in both conditions. Table 1 shows for the monopolar condition that the signed  $r_{PLV}^2$  was negative for most subjects, while the signed  $r_{BP}^2$  was positive. A repeated ANOVA based on the  $r^2$  values showed that there was a significant interaction between conditions (e.g., monopolar and Laplacian) and features (e.g., BP, PLV, and their combination) ( $F(1.2524, 21.2908) = 19.9, p < 0.0001$  corrected from  $F(2, 34) = 19.9, p < 0.0001$ ).

With monopolar data, Tukey’s post hoc statistic tests show that the combination of PLV and BP was significantly better than either BP or PLV because  $r_{CF}^2$  was greater than  $r_{BP}^2$  and  $r_{PLV}^2$ , ( $p < 0.0014$  and  $p < 0.037$ , respectively). There was no significant difference between  $r_{BP}^2$  and  $r_{PLV}^2$  ( $0.097$  vs  $0.124, p = 0.81$ ), showing that the coupling between C3 and FCz had similar target prediction ability as the BP feature from the C3 electrode. These results further support the contention that PLV between C3 and FCz was not entirely due to volume conduction, but rather that it was probably due at least in part to real long-range synchrony. Furthermore, in the monopolar condition, BP and PLV were unique features whose combination resulted in better target prediction than either alone.

Target prediction effects for PLV between C3 and FCz were largely eliminated by the use of the Laplacian ( $r_{PLV}^2 = 0.044$ ). Tukey’s post hoc tests show that  $r_{PLV}^2$

(Laplacian condition) was significantly smaller than  $r_{BP}^2$  (Laplacian condition) ( $0.044$  vs  $0.214, p < 0.0001$ ) and was significantly smaller than  $r_{PLV}^2$  (monopolar condition) ( $0.044$  vs  $0.124, p < 0.012$ ), demonstrating that  $r_{PLV}^2$  was largely eliminated in the Laplacian condition. In addition, combining PLV with BP did not improve the  $r_{CF}^2$  compared with  $r_{BP}^2$  ( $0.215$  vs  $0.224$ ) in the Laplacian condition. Thus, after applying the large Laplacian, there was little useful information in PLV beyond that in BP, which is consistent with the smaller PLV with no significant difference for task 1 and task 2 (Fig. 2b) and the flatter probability distribution at zero-phase difference in Fig. 2d.

Tukey’s post hoc statistic also showed that there was no significant difference between  $r_{BP}^2$  in Laplacian condition and  $r_{CF}^2$  in monopolar condition ( $0.215$  vs  $0.195$ ),  $r_{CF}^2$  in Laplacian and monopolar conditions ( $0.224$  vs  $0.195$ ). It would thus appear that the large Laplacian signal combines amplitude and phase information in the BP feature and eliminates effects for the PLV feature.

### 3.3 Bipolar derivation effects

Given that the effects of the large Laplacian are probability due to the combination of information from BP and PLV, it would be instructive to study the simplest spatial filter [37], a bipolar derivation using the phase-coupled areas (e.g., C3–FCz). A one-way repeated ANOVA comparing

**Table 1** The signed  $r^2$  values based on amplitude feature at C3 (signed  $r_{BP}^2$ ), PLV between C3 and FCz (signed  $r_{PLV}^2$ ) and the  $r^2$  values based on their combined feature ( $r_{CF}^2$ ) for task 2 versus task 1 in monopolar and Laplacian condition

Subject	Monopolar condition			Laplacian condition		
	$r_{BP}^2$	$r_{PLV}^2$	$r_{CF}^2$	$r_{BP}^2$	$r_{PLV}^2$	$r_{CF}^2$
1	0.148	-0.034	0.205	0.235	-0.027	0.240
2	0.088	-0.209	0.309	0.328	0.010	0.329
3	0.167	-0.112	0.200	0.017	0.006	0.034
4	0.028	0.156	0.160	-0.374	0.045	0.409
5	0.168	-0.278	0.364	0.399	-0.178	0.438
6	0.065	-0.014	0.092	0.023	0.015	0.044
7	0.005	0.042	0.042	-0.012	-0.002	0.013
8	0.068	-0.108	0.132	0.154	0.016	0.154
9	0.134	-0.093	0.264	0.339	0.020	0.341
10	0.001	0.113	0.113	-0.103	-0.031	0.104
11	0.001	-0.002	0.004	0.000	0.006	0.006
12	0.005	-0.018	0.029	0.228	0.000	0.230
13	0.564	-0.441	0.614	0.661	0.127	0.677
14	0.091	-0.202	0.318	0.323	0.060	0.327
15	0.000	-0.029	0.033	-0.004	-0.005	0.007
16	0.011	-0.003	0.018	-0.025	-0.017	0.030
17	0.063	-0.121	0.201	0.170	0.000	0.171
18	0.134	-0.265	0.406	0.466	0.220	0.478
Mean	0.097	-0.090	0.195	0.157	0.015	0.224

the  $r_{BP}^2$  of C3 channel in three conditions (e.g., monopolar, Laplacian, bipolar) resulted in a significant effect of condition ( $F(1.319, 22.423) = 13.39, p < 0.0006$  with Greenhouse–Geisser correction) as illustrated in Fig. 4. Tukey's post hoc test shows that there was no significant difference between  $r_{BP}^2$  of C3–FCz (bipolar condition) and C3 (Laplacian condition) ( $p = 0.76$ ) and that both were significantly different from that of C3 (monopolar condition) ( $p < 0.0007$  and  $p < 0.0001$ , respectively). Since Table 1 shows that the Laplacian is likely to combine both amplitude and phase features into a single amplitude feature and eliminate the target prediction information in phase, we suggest that the bipolar channel C3–FCz has similar effects.

## 4 Discussion

### 4.1 Volume conduction and zero-phase coupling

The present study found an increase in PLV between C3 and FCz, at the same time that spectral amplitude decreased at C3 and FCz. This coupling is consistent with the results of several prior studies [1, 38, 48]. However, a local average reference was applied before computing PLV in two studies [1, 38] and a large Laplacian was used in another [48]. Thus, these studies did not examine data without applying spatial filters (e.g., monopolar data). Moreover, none of these prior studies describe zero-phase coupling or volume conduction between the electrodes overlying the SMA and M1 areas.

Wang et al. [44] compared bipolar channels between C3–FCz and C4–FCz to the use of monopolar or CAR-referenced signals for discriminating between motor imagination of right- and left-hand movement. They found that both FCz-referenced and CAR-referenced signals were better than monopolar recordings. These results are consistent with those of the present study. However, the present results extend these findings by showing that these results are due to the combined effects of amplitude modulation and phase coupling rather than effects of opposite modulations of amplitude or reduction of alpha activity unrelated to the task as suggested by Lou et al. [19]. In addition, we have documented the anatomical specificity of these phase relationships (Fig. 3). Finally, our results show that the effects of electrode spacing with the surface Laplacian transform involves phase effects.

Krusienski et al. [15] discussed zero-phase difference between coupled channels at mu- and beta-rhythm bands, but they considered only a limited number of channels. For instance, FC1 and FCz channels were not included as coupled channels when computing PLV. The present study

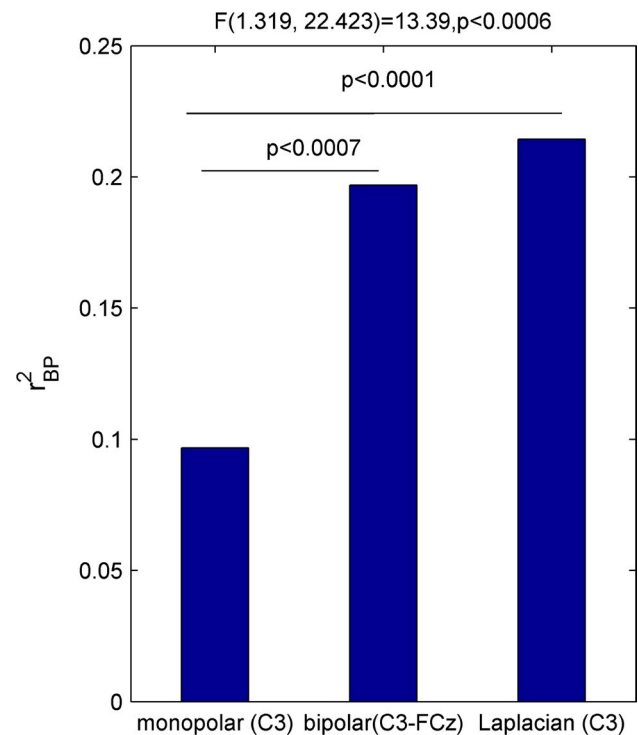


**Fig. 4** The  $r_{BP}^2$  value for prediction of target position of monopolar C3, bipolar C3–FCz and C3 after spatial filtered by Laplacian in the frequency range between 10 and 15 Hz ( $F(1.319, 22.423) = 13.39, p < 0.0006$  with Greenhouse–Geisser correction). Post hoc statistic tests show that there is no significant difference between  $r_{BP}^2$  in bipolar and Laplacian condition. However, both of them are significantly larger than that in monopolar condition

documents zero-phase coupling between electrodes overlying M1 and SMA in monopolar data during SMR control tasks. Moreover, we provide evidence that this coupling is not due solely to volume conduction, but is the result of a contribution from long-range phase synchrony.

Andrew and Pfurtscheller [3] found that a “local average reference” derivation (i.e., a Laplacian derivation) eliminated the increase in coupling with movement between C3 and C4 observe with nose reference data (i.e., monopolar condition). They interpreted this effect of the Laplacian as being due to the removal of volume conducted activity from posterior visual areas and suggested that the derived signals better reflected the activity of the underlying cortical generators. The results of the present study argue against this interpretation. There are two findings from the present study that suggest the coupling with approximately zero-phase difference between C3 and FCz is not due entirely to volume conduction. First, as illustrated in the topographies shown in Fig. 1, phase locking is maximal at C3 and FCz and occurs to a lesser extent in channels between these two sites. Effects due to volume conduction should produce a graded decrease in all directions. Second, these spatial

effects (illustrated in Fig. 3) show differential task-related modulation of PLV at anterior and posterior electrodes in addition to greater modulation at anterior electrodes closer to the midline. All these findings are contrary to expectations that volume conduction should produce a positive association of amplitude and PLV [3, 7].

#### 4.2 Opposite modulation between BP and PLV

According to Mylonas et al. [27], phase synchronization serves as a macroscopic binding mechanism and phase desynchronization reflects the suppression of functional binding in order to accomplish a task. If the BP feature at any given channel is the reflection of the phase synchronization between elements in the immediate vicinity of the electrode, then Fig. 5 provides a model that can explain the opposite modulation between BP and PLV. In order to produce synchronous activity that is recorded at the surface many elements in the vicinity of an electrode must be coupled near zero phase. Otherwise, the activity of these elements recorded at a distance will cancel out. Thus, panel (a) in Fig. 5 shows strong coupling between local elements. In Fig. 5 panel (b), local coupling at zero phase is reduced, producing an ERD. However, coupling at a distant site increases, resulting in an increase in PLV. Thus, Fig. 5 illustrates a possible scenario for how the long-distance functional binding (PLV) between C3 and FCz and BP of C3 changes in opposite directions as observed in this paper. Essentially local coupling is reduced while at the same time distant coupling increases.

#### 4.3 Spatial filters

Spatial filter operations are often applied to improve the SNR of a BCI that uses mu and beta rhythms [22]. McFarland [20] and McFarland et al. [22] compared different

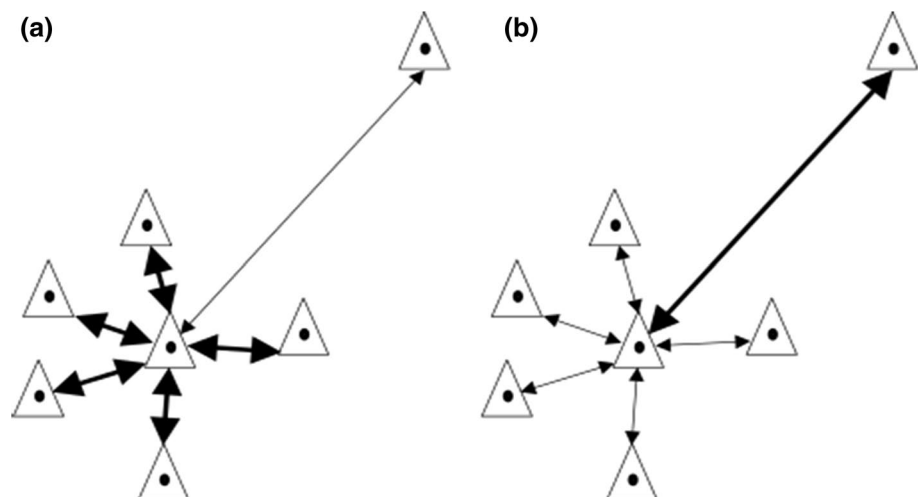
spatial filters and found that both large Laplacian and CAR could provide a higher SNR than either small Laplacian (with a distance of 3 cm) or a monopolar derivation. McFarland [20] concluded that the large Laplacian can reduce spatial noise [22] and constrain potential sources of the signal [40]. This is consistent with the present results where BP at C3 with large Laplacian data (Fig. 1 top right panel) produced a larger ERD than that with monopolar data (Fig. 1 top left panel,  $r_{BP}^2$  in monopolar and Laplacian condition in Table 1). However, McFarland [20] did not consider phase effects.

In the present study, when a large Laplacian was applied, the probability distribution of phase relationships between C3 and FCz was markedly altered (Fig. 2d vs Fig. 2c). Moreover, the large Laplacian appears to combine amplitude and phase information into a single amplitude feature, resulting in little information remaining in PLV for target prediction (Table 1). The results of the present study demonstrate potential problems with using spatial filters to examine PLV.

Tenke and Kayser [41] argued for the use of the surface Laplacian in studies of EEG phase relationships (e.g., coherence). They support this assertion with the results of a simulation based on a 4-sphere head model with pure cosine or sine waveform at one specific frequency. However, actual EEG signals are probably the result of a mixture of many sources that may have complex phase relationships that were not evaluated in these simulations.

The bipolar derivation between C3 and FCz may have considerable potential for use as a control signal. The bipolar channel C3–FCz produces a significantly better  $r_{BP}^2$  than the monopolar channel at C3 and has similar target prediction ability as that of C3 with a large Laplacian. At the same time, the bipolar channel requires fewer electrodes and is thus more efficient and less susceptible to effects of occasional noisy channels. The enhancement of the signal

**Fig. 5** Local reduction and distal increase in connectivity with event-related desynchronization. In **a** the neural elements near an electrode (e.g., C3) show strong bi-directional coupling while elements at a distance show less coupling. In **b** coupling is reduced locally, producing an event-related desynchronization. At the same time, coupling with distant elements increases (e.g., neural units in the vicinity of FCz)



with a bipolar derivation is not due to the amplitude based “focal ERD/surround ERS” [32] effect (there are also amplitude decreases in task 2 for FCz channel, Fig. 2a monopolar). Rather, the enhancement appears to be due to the fact that the bipolar channel combines phase and amplitude information in a manner similar to the large Laplacian. Thus, the bipolar derivation (e.g., C3–FCz) combines the information available in amplitude and phase features with fewer channels than that required to compute large Laplacian. The use of bipolar channels provides a very efficient way to optimize the recording setup since only two signal electrodes and the ground need to be attached. In contrast, the Laplacian generally requires five electrodes to record the signals as well as a reference and ground. It may also be important to consider that other spatial filters, such as those produced by common spatial patterns or independent components analysis [14] may also combine amplitude and phase information. Knowledge of potential phase effects on spatial filters may ultimately aid in the design of better spatial filters.

It is a common practice to use Fz, FCz or Cz as a reference when recording EEG for investigations of neurophysiological phenomena [26, 42] including studies examining coherence [25]. The present results suggest that interpretations could potentially be biased since all recordings are then bipolar with respect to this reference.

#### 4.4 Implications and limitations

Several authors have asserted that zero-phase coupling is not meaningful because it is due simply to volume conduction [28, 31]. Indeed, these authors propose that indices of coupling completely eliminate effects at zero lag. Others have suggested that coupling at a zero-phase difference between channels might reflect real long-distance phase-locking [4, 12]. Using simulations, Gollo et al. [12] found that zero-phase coupling may be indicative of a resonance pair of mutually coupled nodes or of a third source providing a common drive. Thus, there are theoretical reasons for not summarily dismissing coupling with zero-phase lag.

The present study is based on EEG data after ten sessions of training on a BCI task. The degree of training might affect the degree of elimination of PLV by spatial filtering. For example, the results in [45] shows that after spatial filtering by CAR, there is still additional information in PLV between electrodes in M1 and that in SMA areas for task prediction for EEG data with not much training. Thus, it would be interesting to study whether large Laplacian has the similar effects on PLV feature for untrained EEG data from motor imaginary tasks. It is also interesting to study whether other spatial filters, for instance, common spatial patterns or independent components analysis, have similar effects on PLV feature.

## 5 Conclusion

This study found that coupling between C3 and FCz at approximately zero-phase delay provided information about target location in addition to that provided by amplitude. The zero-phase coupling was likely due to long-range synchronization because amplitude and coupling were modulated in opposite directions by target position. When large Laplacian spatial filtering was applied these phase effects were eliminated. This likely indicates that spatial filters may combine both amplitude and phase information. Amplitude and phase information can more efficiently be combined by use of a bipolar derivation.

**Acknowledgements** This work was supported in part by the National Institutes of Health (NIH) (Grants HD30146 46) (NCMRR/NICHHD), EB00856 (NIBIB &NINDS), National “111” Project (B08036) and in part by the China Scholarship Council. The authors would like to thank Jonathan Carp and Li Zhang for their helpful comments on an earlier version of this paper.

## References

1. Andrew C, Pfurtscheller G (1996) Event-related coherence as a tool for studying dynamic interaction of brain regions. *Electroencephalogr Clin Neurophysiol* 98:144–148. doi:[10.1016/0013-4694\(95\)00228-6](https://doi.org/10.1016/0013-4694(95)00228-6)
2. Andrew C, Pfurtscheller G (1997) On the existence of different alpha band rhythms in the hand area of man. *Neurosci Lett* 222:103–106. doi:[10.1016/S0304-3940\(97\)13358-4](https://doi.org/10.1016/S0304-3940(97)13358-4)
3. Andrew C, Pfurtscheller G (1996) Dependence of coherence measurements on EEG derivation type. *Med Biol Eng Comput* 34:232–238. doi:[10.1007/BF02520079](https://doi.org/10.1007/BF02520079)
4. Bastos AM, Vezoli J, Fries P (2015) Communication through coherence with inter-areal delays. *Curr Opin Neurobiol* 31:173–180. doi:[10.1016/j.conb.2014.11.001](https://doi.org/10.1016/j.conb.2014.11.001)
5. Bayraktaroglu Z, von Carlowitz-Ghori K, Curio G, Nikulin VV (2013) It is not all about phase: amplitude dynamics in corticomuscular interactions. *NeuroImage* 64:496–504. doi:[10.1016/j.neuroimage.2012.08.069](https://doi.org/10.1016/j.neuroimage.2012.08.069)
6. Brunner C, Scherer R, Graimann B, Supp G, Pfurtscheller G (2006) Online control of a brain–computer interface using phase synchronization. *IEEE Trans Biomed Eng* 53:2501–2506. doi:[10.1109/TBME.2006.881775](https://doi.org/10.1109/TBME.2006.881775)
7. Celka P (2007) Statistical analysis of the phase-locking value. *IEEE Signal Process Lett* 14:577–580. doi:[10.1109/LSP.2007.896142](https://doi.org/10.1109/LSP.2007.896142)
8. Chawla D, Friston KJ, Lumer ED (2001) Zero-lag synchronous dynamics in triplets of interconnected cortical areas. *Neural Netw* 14:727–735. doi:[10.1016/S0893-6080\(01\)00043-0](https://doi.org/10.1016/S0893-6080(01)00043-0)
9. Daffertshofer A, van Wijk BCM (2011) On the influence of amplitude on the connectivity between phases. *Front Neuroinformatics* 5:6. doi:[10.3389/fninf.2011.00006](https://doi.org/10.3389/fninf.2011.00006)
10. Flandrin P, Rilling G, Goncalves P (2004) Empirical mode decomposition as a filter bank. *IEEE Signal Process Lett* 11:112–114. doi:[10.1109/LSP.2003.821662](https://doi.org/10.1109/LSP.2003.821662)
11. Florian G, Andrew C, Pfurtscheller G (1998) Do changes in coherence always reflect changes in functional coupling?

- Electroencephalogr Clin Neurophysiol 106:87–91. doi:[10.1016/S0013-4694\(97\)00105-3](https://doi.org/10.1016/S0013-4694(97)00105-3)
12. Gollo LL, Mirasso C, Sporns O, Breakspear M (2014) Mechanisms of zero-lag synchronization in cortical motifs. *PLoS Comput Biol* 10:e1003548. doi:[10.1371/journal.pcbi.1003548](https://doi.org/10.1371/journal.pcbi.1003548)
  13. Huang NE, Shen Z, Long SR, Wu MC, Shih HH, Zheng Q, Yen N-C, Tung CC, Liu HH (1998) The empirical mode decomposition and the Hilbert spectrum for nonlinear and non-stationary time series analysis. *Proc R Soc Lond Math Phys Eng Sci* 454:903–995. doi:[10.1098/rspa.1998.0193](https://doi.org/10.1098/rspa.1998.0193)
  14. Krusienski DJ (2009) A method for visualizing independent spatio-temporal patterns of brain activity. *EURASIP J Adv Signal Process* 2009:948961. doi:[10.1155/2009/948961](https://doi.org/10.1155/2009/948961)
  15. Krusienski DJ, McFarland DJ, Wolpaw JR (2012) Value of amplitude, phase, and coherence features for a sensorimotor rhythm-based brain–computer interface. *Brain Res Bull* 87:130–134. doi:[10.1016/j.brainresbull.2011.09.019](https://doi.org/10.1016/j.brainresbull.2011.09.019)
  16. Lachaux JP, Rodriguez E, Martinerie J, Varela FJ (1999) Measuring phase synchrony in brain signals. *Hum Brain Mapp* 8:194–208
  17. Le Van Quyen M, Foucher J, Lachaux J-P, Rodriguez E, Lutz A, Martinerie J, Varela FJ (2001) Comparison of Hilbert transform and wavelet methods for the analysis of neuronal synchrony. *J Neurosci Methods* 111:83–98. doi:[10.1016/S0165-0270\(01\)00372-7](https://doi.org/10.1016/S0165-0270(01)00372-7)
  18. Leocani L, Toro C, Manganotti P, Zhuang P, Hallett M (1997) Event-related coherence and event-related desynchronization/synchronization in the 10 Hz and 20 Hz EEG during self-paced movements. *Electroencephalogr Clin Neurophysiol Potentials Sect* 104:199–206. doi:[10.1016/S0168-5597\(96\)96051-7](https://doi.org/10.1016/S0168-5597(96)96051-7)
  19. Lou B, Hong B, Gao X, Gao S (2008) Bipolar electrode selection for a motor imagery based brain–computer interface. *J Neural Eng* 5:342. doi:[10.1088/1741-2560/5/3/007](https://doi.org/10.1088/1741-2560/5/3/007)
  20. McFarland DJ (2015) The advantages of the surface Laplacian in brain–computer interface research. *Int J Psychophysiol* 97:271–276. doi:[10.1016/j.ijpsycho.2014.07.009](https://doi.org/10.1016/j.ijpsycho.2014.07.009)
  21. McFarland DJ, Lefkowitz AT, Wolpaw JR (1997) Design and operation of an EEG-based brain–computer interface with digital signal processing technology. *Behav Res Methods Instrum Comput* 29:337–345. doi:[10.3758/BF03200585](https://doi.org/10.3758/BF03200585)
  22. McFarland DJ, McCane LM, David SV, Wolpaw JR (1997) Spatial filter selection for EEG-based communication. *Electroencephalogr Clin Neurophysiol* 103:386–394. doi:[10.1016/S0013-4694\(97\)00022-2](https://doi.org/10.1016/S0013-4694(97)00022-2)
  23. McFarland DJ, Sarnacki WA, Vaughan TM, Wolpaw JR (2005) Brain–computer interface (BCI) operation: signal and noise during early training sessions. *Clin Neurophysiol* 116:56–62. doi:[10.1016/j.clinph.2004.07.004](https://doi.org/10.1016/j.clinph.2004.07.004)
  24. McFarland DJ, Wolpaw JR (2003) EEG-based communication and control: speed–accuracy relationships. *Appl Psychophysiol Biofeedback* 28:217–231. doi:[10.1023/A:1024685214655](https://doi.org/10.1023/A:1024685214655)
  25. Miskovic V, Schmidt LA, Boyle M, Saigal S (2009) Regional electroencephalogram (EEG) spectral power and hemispheric coherence in young adults born at extremely low birth weight. *Clin Neurophysiol* 120:231–238. doi:[10.1016/j.clinph.2008.11.004](https://doi.org/10.1016/j.clinph.2008.11.004)
  26. Moll K, Hasko S, Groth K, Bartling J, Schulte-Körne G (2016) Letter-sound processing deficits in children with developmental dyslexia: an ERP study. *Clin Neurophysiol* 127:1989–2000. doi:[10.1016/j.clinph.2016.01.005](https://doi.org/10.1016/j.clinph.2016.01.005)
  27. Mylonas DS, Siettos CI, Evdokimidis I, Papanicolaou AC, Smyrnis N (2015) Modular patterns of phase desynchronization networks during a simple visuomotor task. *Brain Topogr* 29:118–129. doi:[10.1007/s10548-015-0451-5](https://doi.org/10.1007/s10548-015-0451-5)
  28. Nolte G, Bai O, Wheaton L, Mari Z, Vorbach S, Hallett M (2004) Identifying true brain interaction from EEG data using the imaginary part of coherency. *Clin Neurophysiol* 115:2292–2307. doi:[10.1016/j.clinph.2004.04.029](https://doi.org/10.1016/j.clinph.2004.04.029)
  29. Nunez PL, Silberstein RB, Shi Z, Carpenter MR, Srinivasan R, Tucker DM, Doran SM, Cadusch PJ, Wijesinghe RS (1999) EEG coherency II: experimental comparisons of multiple measures. *Clin Neurophysiol* 110:469–486. doi:[10.1016/S1388-2457\(98\)00043-1](https://doi.org/10.1016/S1388-2457(98)00043-1)
  30. Nunez PL, Srinivasan R, Westdorp AF, Wijesinghe RS, Tucker DM, Silberstein RB, Cadusch PJ (1997) EEG coherency: I: statistics, reference electrode, volume conduction, Laplacians, cortical imaging, and interpretation at multiple scales. *Electroencephalogr Clin Neurophysiol* 103:499–515. doi:[10.1016/S0013-4694\(97\)00066-7](https://doi.org/10.1016/S0013-4694(97)00066-7)
  31. Peraza LR, Asghar AUR, Green G, Halliday DM (2012) Volume conduction effects in brain network inference from electroencephalographic recordings using phase lag index. *J Neurosci Methods* 207:189–199. doi:[10.1016/j.jneumeth.2012.04.007](https://doi.org/10.1016/j.jneumeth.2012.04.007)
  32. Pfurtscheller G, Lopes da Silva FH (1999) Event-related EEG/MEG synchronization and desynchronization: basic principles. *Clin Neurophysiol* 110:1842–1857. doi:[10.1016/S1388-2457\(99\)00141-8](https://doi.org/10.1016/S1388-2457(99)00141-8)
  33. Rappelsberger P, Pfurtscheller G, Filz O (1994) Calculation of event-related coherence—a new method to study short-lasting coupling between brain areas. *Brain Topogr* 7:121–127. doi:[10.1007/BF01186770](https://doi.org/10.1007/BF01186770)
  34. Schalk G, McFarland DJ, Hinterberger T, Birbaumer N, Wolpaw JR (2004) BCI2000: a general-purpose brain–computer interface (BCI) system. *IEEE Trans Biomed Eng* 51:1034–1043. doi:[10.1109/TBME.2004.827072](https://doi.org/10.1109/TBME.2004.827072)
  35. Sharbrough F, Chatrian CE, Lesser RP, Luders H, Nuwer M and Picton TW (1991) American electroencephalographic society guidelines for standard electrode position nomenclature. *J Clin Neurophysiol* 8:200–202
  36. Sheikh H, McFarland DJ, Sarnacki WA, Wolpaw JR (2003) Electroencephalographic(EEG)-based communication: EEG control versus system performance in humans. *Neurosci Lett* 345:89–92. doi:[10.1016/S0304-3940\(03\)00470-1](https://doi.org/10.1016/S0304-3940(03)00470-1)
  37. Simpson EV, Ideker RE, Cabo C, Yabe S, Zhou X, Melnick SB, Smith WM (1993) Evaluation of an automatic cardiac activation detector for bipolar electrograms. *Med Biol Eng Comput* 31:118–128. doi:[10.1007/BF02446669](https://doi.org/10.1007/BF02446669)
  38. Spiegler A, Graitmann B, Pfurtscheller G (2004) Phase coupling between different motor areas during tongue-movement imagery. *Neurosci Lett* 369:50–54. doi:[10.1016/j.neulet.2004.07.054](https://doi.org/10.1016/j.neulet.2004.07.054)
  39. Stam CJ, Nolte G, Daffertshofer A (2007) Phase lag index: assessment of functional connectivity from multi channel EEG and MEG with diminished bias from common sources. *Hum Brain Mapp* 28:1178–1193. doi:[10.1002/hbm.20346](https://doi.org/10.1002/hbm.20346)
  40. Tenke CE, Kayser J (2012) Generator localization by current source density (CSD): implications of volume conduction and field closure at intracranial and scalp resolutions. *Clin Neurophysiol* 123:2328–2345. doi:[10.1016/j.clinph.2012.06.005](https://doi.org/10.1016/j.clinph.2012.06.005)
  41. Tenke CE, Kayser J (2015) Surface Laplacians (SL) and phase properties of EEG rhythms: simulated generators in a volume-conduction model. *Int J Psychophysiol* 97:285–298. doi:[10.1016/j.ijpsycho.2015.05.008](https://doi.org/10.1016/j.ijpsycho.2015.05.008)
  42. Vollebregt MA, Zumer JM, ter Huurne N, Buitelaar JK, Jensen O (2016) Posterior alpha oscillations reflect attentional problems in boys with attention deficit hyperactivity disorder. *Clin Neurophysiol* 127:2182–2191. doi:[10.1016/j.clinph.2016.01.021](https://doi.org/10.1016/j.clinph.2016.01.021)
  43. Wang Y, Hong B, Gao X, Gao S (2006) Phase synchrony measurement in motor cortex for classifying single-trial EEG during motor imagery. *IEEE*, pp 75–78
  44. Wang Y, Hong B, Gao X, Gao S (2007) Design of electrode layout for motor imagery based brain–computer interface. *Electron Lett* 43:557. doi:[10.1049/el:20070563](https://doi.org/10.1049/el:20070563)

45. Wei Q, Wang Y, Gao X, Gao S (2007) Amplitude and phase coupling measures for feature extraction in an EEG-based brain-computer interface. *J Neural Eng* 4:120. doi:[10.1088/1741-2560/4/2/012](https://doi.org/10.1088/1741-2560/4/2/012)
46. Witham CL, Wang M, Baker SN (2007) Cells in somatosensory areas show synchrony with beta oscillations in monkey motor cortex. *Eur J Neurosci* 26:2677–2686. doi:[10.1111/j.1460-9568.2007.05890.x](https://doi.org/10.1111/j.1460-9568.2007.05890.x)
47. Wolpaw JR, Birbaumer N, McFarland DJ, Pfurtscheller G, Vaughan TM (2002) Brain-computer interfaces for communication and control. *Clin Neurophysiol* 113:767–791. doi:[10.1016/S1388-2457\(02\)00057-3](https://doi.org/10.1016/S1388-2457(02)00057-3)
48. Zhou Z, Wan B, Ming D, Qi H (2010) A novel technique for phase synchrony measurement from the complex motor imaginary potential of combined body and limb action. *J Neural Eng* 7:46008. doi:[10.1088/1741-2560/7/4/046008](https://doi.org/10.1088/1741-2560/7/4/046008)



**Wenjuan Jian, B.S.** is currently pursuing the Ph.D. degree in Chongqing University and a visiting scientist in Wadsworth Center, Albany. Her research interests include motor imagery-based brain-computer interface (BCI) and EEG signal processing.



**Minyou Chen, Ph.D.** is currently a Full Professor with Chongqing University. His current research interests include Brain-computer Interface (BCI), intelligent modeling and control. He has authored or co-authored over 180 papers.



**Dennis J. McFarland, Ph.D.** is a senior Research Scientist with the Wadsworth Center for Laboratories and Research, New York State Department of Health, Albany. His research interests include the development of EEG-based communication and auditory perception.